

# A geothermally influenced wetland containing unconsolidated geochemical sediments

A. Channing, D. Edwards, and S. Sturtevant

**Abstract:** Hot spring waters flowing from Porkchop Geysir, Norris Geysir Basin, Yellowstone National Park, USA, enter a shallow wetland basin and precipitate opal-A silica particulate. Particulate formation by chemical (rather than biochemical) and colloidal mechanisms is suggested by floc- and shard-like particle morphologies comprising opal-A silica nanospheres and microspheres of colloidal dimensions and precipitation from waters with opaque milky-blue colouration, indicative of aqueous silica-sol conditions. Sediment accumulates in the wetland at a rate of ca. 20–25 mm/year, is unconsolidated, and massive to diffusely bedded to laminated. Post depositional features include soft sediment deformation and scouring, and in drying conditions, relatively deep desiccation. Establishment of geochemically dominated wetland sedimentation is favoured where alkali-chloride hot spring fluids of circum neutral to basic pH and high silica concentration discharge to and cool (to < ca. 35 °C) within topographic depressions that receive only small volumes of non-hot spring water. Local wetland vegetation, which is composed of hydrophytes, halophytes, and alkali-tolerant species more typical of coastal wetlands, colonizes the soft wetland substrate and may be relatively quickly buried by rapid sediment accumulation. Prior to the evolution of the diatom silica-sink, geothermal wetlands containing geochemically precipitated silica sediments may have been much more common and widespread. Rhizoliths, chert nodules with organic cores, scour fabrics, soft sediment deformation, desiccation cracks, and massive to diffuse bedding preserved in Palaeozoic geothermal environments may all be evidence of ancient unconsolidated geochemical sediments and geothermal wetland conditions.

**Résumé :** Les eaux de sources thermales s'écoulant du geysir Porkchop, dans le bassin de geysers Norris du parc national Yellowstone aux États-Unis, entrent dans un bassin marécageux peu profond et précipitent de la silice particulière sous forme d'opale-A. La formation des particules par des mécanismes chimiques (plutôt que biochimiques) et colloïdaux est suggérée par la morphologie des particules, sous forme de floes et d'épaufrures, qui comprennent des nanosphères de silice opale-A et des microsphères de dimension colloïdale ainsi que des précipitations à partir d'eaux à coloration opaque bleu laiteux, indiquant des conditions aqueuses de sol de silice. Les sédiments s'accumulent dans le marécage à un taux d'environ 20–25 mm/a, ils ne sont pas consolidés et sont sous forme de lits massifs à diffus à laminés. Les caractéristiques post-dépositionnelles comprennent une déformation des sédiments mous et de l'affouillement et, dans des conditions de sécheresse, une dessiccation relativement profonde. Dans les marécages, l'établissement d'une sédimentation dominée par la géochimie est favorisé là où des fluides de chlorures alcalins de sources thermales, ayant un pH de presque neutre à basique et de hautes concentrations en silice, se déchargent vers des dépressions topographiques qui ne reçoivent que de faibles quantités d'eau ne provenant pas de sources thermales et y refroidissent (à des températures inférieures à environ 35 °C). La végétation locale des marécages, composée d'hydrophytes, d'halophytes et d'espèces tolérant les alcalis plus typiques des marécages côtiers, colonise le substratum mou du marécage et peut être relativement rapidement ensevelie par une accumulation rapide de sédiments. Avant l'évolution de la prise de la silice par les diatomées, les marécages géothermiques contenant des sédiments de silice précipités géochimiquement pourraient avoir été beaucoup plus communs et étendus. Les traces calcifiées de racines, les nodules de chailles présentant des noyaux organiques, du matériel d'affouillement, la déformation de sédiments mous, les fissures de dessiccation et des lits massifs à diffus préservés dans les environnements géothermiques du Paléozoïque peuvent tous être des évidences d'anciens sédiments géochimiques non consolidés et de conditions de marécages géothermiques.

[Traduit par la Rédaction]

Received 17 July 2003. Accepted 15 April 2004. Published on the NRC Research Press Web site at <http://cjes.nrc.ca> on 16 July 2004.

Paper handled by Associate Editor G.R. Dix.

**A. Channing<sup>1</sup> and D. Edwards.** School of Earth, Ocean and Planetary Sciences, Cardiff University, Cathays Park, Cardiff, Wales, CF10 3YE, United Kingdom.

**S. Sturtevant.** 5225 Alkali Creek Rd., Billings, Montana, MT 59106–9511, USA.

<sup>1</sup>Corresponding author: (e-mail: [channinga@cardiff.ac.uk](mailto:channinga@cardiff.ac.uk)).

## Introduction

Most silica-depositing hot springs precipitate silica to form hard, structurally robust, and relatively durable subaqueous and subaerial sinter deposits. A suite of biotic (e.g., Guidry and Chafetz 2003a, 2003b) and abiotic mechanisms, e.g., rapid cooling (e.g., Guidry and Chafetz 2002; Yee et al. 2003), evaporation and evaporative wicking (e.g., Hinman and Lindstrom 1996), low pH or rapid pH change (e.g., Rimstidt and Cole 1983; Fournier 1985), and cation effects (e.g., Rimstidt and Cole 1983) have been suggested to mediate opal-A silica deposition. In the silica-supersaturated aquatic environments associated with alkali-chloride, high silica hot springs silica precipitation can be predicted by equilibrium thermodynamic principles (e.g., Mountain et al. 2003; Yee et al. 2003), active biological mediation of silica nucleation, polymerization, and precipitation does not, therefore, appear to be a requirement for silica deposition.

Proximal to the vents of silica-depositing springs opaline silica accretes to form positive topographic features, such as sinter mounds and aprons. Areas of negative topographic relief within or at the margins of geothermal basins often form shallow wetland or aquatic environments. Distal wetlands form extensive areas of low-temperature, geothermally influenced environment at the margins of many active hot spring basins (e.g., Weed 1889; Walter 1976; Channing 2001, 2003; Trewin et al. 2003).

Sedimentation in Holocene geothermally influenced wetlands is dominated by the input of biogenic silica from diatom frustules. At Upper Geysir Basin, Yellowstone National Park, diatomites of Holocene age have accumulated to depths of several metres (Muffler et al. (1982), report between 0.3 and 4.5 m of diatomite), indicating potentially rapid accretion rates. Despite silica biomineralization by diatoms, waters in an area of accumulating diatomite in Elk Park south of Norris Geysir Basin, Yellowstone (Figs. 1A–1C) are supersaturated with respect to crystalline (quartz saturation index (SI) = 1.47) and amorphous (SiO<sub>2</sub> amorphous SI = 0.30) silica phases, with recorded dissolved silica concentrations of 270–280 mg/kg at ca. 35 °C (Channing 2001). Below the ca. 35–40 °C isotherm (Walter and Des Marais 1993), geothermally influenced wetlands around silica depositing springs are a major habitat for abundant hydrophytic, halophytic, and alkali tolerant vascular plants (Channing 2001, 2003; Trewin et al. 2003). Interaction of the silica-supersaturated waters with the wetland vegetation means that geothermal wetlands are a major, if not *the* major, environment of higher plant silicification at present active in Yellowstone (Channing 2001).

Marshes associated with hot spring and sinter deposits of the Drummond Basin, Queensland, Australia (e.g., White et al. 1989; Walter et al. 1996, 1998) provide clear evidence that the geological record of geothermally influenced wetlands extends back at least to the mid Palaeozoic and that the environment was a site of plant silicification. As now, the Drummond Basin wetlands provided habitat for vegetation considered to have grown in semi-aquatic (emergent) conditions with subaqueous root–rhizome systems in waterlogged soil (e.g., Walter et al. 1998). Sedimentological features, including rhizoliths formed around roots in non-detrital silica substrates (Walter et al. 1998), scour fabrics, soft-sediment deformation, e.g., slumps (Walter et al. 1996), desiccation cracks (White

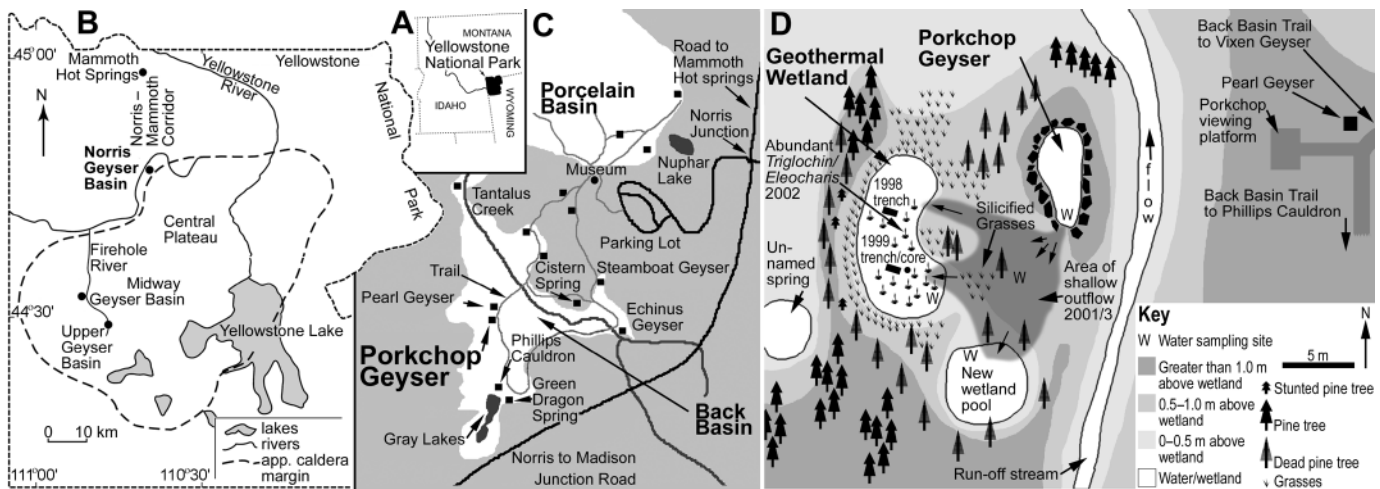
et al. 1989), and massive to diffuse bedding (Walter et al. 1996, 1998), described from the Drummond hot spring deposits may also be attributed to the presence of an opal-A substrate that, like diatomite, was unconsolidated, soft, and mobile. Diatoms, however, have a fossil record that extends only to the late Mesozoic; thus they can have played no part in sedimentation in Drummond Basin wetlands.

The Lower Devonian (Pragian) Rhynie and Windyfield cherts of Aberdeenshire, Scotland (Rice et al. 2002 and references therein) similarly contain abundant evidence of wetland environments (e.g., Channing 2001, 2003; Trewin et al. 2003). Sedimentological features indicative of unconsolidated wetland substrates include nodular chert horizons containing abundant rhizomes–rhizoliths (Powell 1994; Trewin 1994, 1996; Powell et al. 2000), gradational contacts between chert horizons and overlying clastic sediments (Powell 1994; Channing 2001), and metre-scale lenticular bodies of massive to diffusely bedded homogeneous chert (e.g., Channing 2001). Waterlogged soil–substrate conditions are suggested by an absence of red beds, abundance of pyrite and retention in the subsurface of carbon (Powell et al. 2000). Plant growth and preservation in a subaqueous setting is illustrated by Rhynie plants exhibiting exceptional preservation in situ, in pod-like chert lenses, in association with an aquatic fauna and flora, e.g., the crustacean *Lepidocaris*, charophyte alga *Palaeonitella*, and chytrid fungi (Trewin et al. 2003). Comparisons of Rhynie chert colour and porosity (dark-brown to black and impermeable, respectively) with proximal Drummond Basin (Walter et al. 1998) and modern (e.g., Channing 2001) sinter material (light grey–blue to white and porous) allied with the large numbers of well-preserved plants that characterize many Rhynie Chert horizons suggests that fossilisation of the Rhynie flora and fauna occurred predominantly in subaqueous settings at lower temperatures. Taphonomic and anatomical features of the Rhynie plants may also illustrate adaptation or tolerance of wetland conditions. For example, many of the plants have shallow rhizomes rather than deep roots suggesting the presence of a water table at or above the sediment surface. The abundance of plants preserved with erect axes appear to illustrate a resistance to the wilting that is induced by waterlogging of modern plant roots despite the Rhynie plants lacking structural tissues and relying primarily on cell turgor for support (e.g., Powell et al. 2000; Channing 2001). Additionally, many Rhynie plants illustrate detailed arrangements of cells e.g., intercellular air spaces (spongy cortical tissues, sub-stomatal cavities), sunken stomata, and thickened cuticle and cuticular ledges on stomata, which demonstrate high water use efficiency characteristic of water stressed, perhaps brackish to saline aquatic wetland environments (Edwards et al. 1998; Channing 2001, 2003).

The wetlands associated with the Rhynie hot springs are particularly important as they were clearly very favourable environments for silicification and preservation of the Rhynie biota. Channing (2001) and later Trewin et al. (2003) proposed that a suitable analogue environment for formation of the Rhynie chert would most likely be found by investigating permanently wet marshy areas associated with silica precipitating springs. Both references, however, point out that the removal of silica by diatoms in modern environments is a major obstacle to close analogy.

Here we describe an active wetland environment in the

**Fig. 1.** Location maps for (A) Yellowstone National Park, (B) Norris Geyser Basin, (C) Porkchop Geyser and (D) sketch map showing position of Porkchop Geyser, adjacent wetlands, and water and sediment sampling sites.



Back Basin area of Norris Geyser Basin, Yellowstone National Park, which is potentially analogous to hot spring wetlands prior to the late Mesozoic that has accreted unconsolidated sediments via an as yet unconfirmed, but apparently dominantly abiotic mechanism.

## Geographical, geological, and geochemical setting

### Yellowstone National Park

Yellowstone National Park is located in the northwest corner of Wyoming, USA., with western and northern boundaries in the adjacent states of Idaho and Montana (Figs. 1A–1B). Yellowstone has been an active centre of volcanism over the past ca. 2.2 Ma. Three climactic caldera forming silicic pyroclastic eruptions at ca. 2.0, 1.3, and 0.6 Ma punctuate this period (e.g., White et al. 1988). Surface geothermal activity occurs throughout the park, but most of the major geothermal basins, particularly those containing silica-depositing geothermal springs, occur on the Yellowstone Plateau (Fig. 1B) within or adjacent to the 0.6 Ma caldera margin (e.g., Fournier 1989). Norris Geyser Basin (Figs. 1A–1C) is situated just outside the 0.6 Ma caldera margin within a north–south subsidence structure, the Norris–Mammoth Corridor, which focuses rising geothermal fluid flow (e.g., Kharaka et al. 2000). Pleistocene–Holocene glacial and geothermal deposits of the area lie above the ca. 600 Ka Lava Creek Tuff. Evidence in the form of chalcidized (crystallized) sinters that lay beneath deposits of the local early Pinedale glacial episode (Early Wisconsin Glacial) indicates geothermal activity over at least the last ca. 150 Ka (White et al. 1988).

### Porkchop Geyser

The focus of this study, Porkchop Geyser (Universal Transverse Mercator (UTM) Zone 12 grid reference 0523202mE, 4951928mN) and adjacent wetland areas are located in the Back Basin area of Norris Geyser Basin (Figs. 1C–1D; White et al. 1988, pl. 1, grid square F4). A synthesis of recorded vent pool and wetland hydrochemistry (Table 1) and eruption style and frequency (Table 2) illustrate marked variation in hydrothermal activity over the past century.

### Wetland basin

#### Position and geometry

Unconsolidated silica sediments occupy an elliptical depression ca. 5 m × ca. 10 m located ca. 10 m to the west of Porkchop Geyser (Figs. 1D, 2A). Unconsolidated, soft white to grey sediment fills the depression to a maximum observed depth of over 40 cm at the centre of the basin (Fig. 2B). At the basin margin, the sediment thins, creating a deposit of lenticular cross-section. The basin margin lies ca. 1 m topographically below the vent pool of Porkchop Geyser (Figs. 1D, 2A). A relatively steep slope composed (at the surface) of brecciated and brecciated to re-cemented sinter material separates the geyser from the basin (Fig. 2A).

#### Source of water influx

The wetland depression is topographically isolated from all surface sources of geothermal water other than Porkchop Geyser. Sedimentological evidence of the historical influx of silica-rich thermal water from Porkchop Geyser is provided by the thin tongue of sinter, which extends from the southern and western edges of the vent pool into and over the surface of the basin fill (Fig. 2A). The main drainage stream of this area of the Back Basin flows northward in close proximity just to the east of Porkchop Geyser, but is separated from the wetland basin by the linear ridge (geyser mound), on which Porkchop sits (Figs. 1D, 2A). A quiescent unnamed geothermal feature situated to the west of the wetland is separated from the basin by another low linear ridge composed of glacial gravels, kame or altered volcanic products (Fig. 1D).

During the period April 2001 to October 2002, shallow diffuse run off from the southern margin of Porkchop Geyser flowed into the wetland basin plus a newly flooded depression to the south (Figs. 1D, 2A). Standing water with an opaque milky-blue colouration (Fig. 2A), comparable to that observed in Porkchop Geyser's vent during periods when the vent fluids contained polymerized silica (Fig. 2C), filled the basin to a depth of ca. 15 cm. Recorded water temperatures ca. 4 m from the outflow of Porkchop Geyser towards the wetland were 24 °C in mid-April (air temperature ca. 2 °C) and 33 and 38 °C in mid-July and mid-October, respectively. Recorded water temperatures in the wetland pool were 18 °C

**Table 1.** Hydrochemistry of Porkchop Geysir and adjacent wetland pools.

Date <sup>a</sup>	Temp (°C)	pH	Cond. (mS)	Silica (mg/kg)	SI	SI m20	Na	K	Cl	Li	Mg	Ca	SO <sub>4</sub>	HCO <sub>3</sub>	F	Data source
<b>Vent Pool</b>																
1920s	90.5			492	0.18	0.67	417	59	688	6	1	7	40	30		1
08/51	84.5			529	0.25	0.70	439	74	744	8.4	0.2	5.8	38	27	4.9	2
18/9/60	72	7.4		435	0.23	0.61	526	66	860	7.40	0.50	6.40	33	18		3
09/61	72			420	0.22	0.60	512	56	826	6.5	0.7	10.4	76	25	7.5	2
09/62	68			432	0.26	0.61	502	56	760	6.5		8.4	26		7.0	2
09/72	91	7.6		510	0.18	0.68	470	61	780	6.3	0.07	7.0	24.6	30	7.3	2,4
06/75	70			510	0.32	0.68	444	64	712	6.2	0.02	5.3	26	39	6.3	2
0775	92			472	0.15	0.65	433	58	697	6.0	0.04	4.8	43	40	5.8	2
09/84	90			552	0.23	0.72	416	73.5	802	7.3	0.03	4.2	17	48	6.1	2
06/89	92	8.5		741	0.26	0.83	388	91	687	6.6	0.06	3.60	23	62	5.8	2,3
01/90	92			680	0.31	0.81	453	94	676	6.2	0.29	3.5	85	58	6.5	2
1994		8.3														5
06/95	71.3	7.5		582	0.36	0.74	396	80.0	664				24.7	19.6	6.36	6
07/95	86.5	8.0		719	0.34	0.83	388	87.7	661				22.1		6.14	6
08/95	82.8	6.3		616	0.32	0.76	451	84.6	704				27		7.07	6
09/95	78.6	7.4		666	0.38	0.80	495	99.0	760				28.8		7.75	6
08/96	47.3	6.8	2.35													7
Summer 98	41.5	6.6	2.20													8
03/07/03	85.6	8.3	2.95													10
17/07/03	89.5	6.3	2.73													10
<b>Vent pool outflow</b>																
09–10/98	45	6.3	2.82	356	0.33	0.53	398	52.6		8.61	0.03	6.55				8
08–09/1999	46	6.9	2.72	406	0.38	0.58	376	51.6		7.43	0.02	5.60				8
04/02	68.2	7.1	2.76	332	0.14	0.50	401	114.1	640		0.08	5.41	20.9		4.7	9
10/02	81.8	7.9	2.22	329	0.04	0.49	378	110.3	654		0.08	4.42	21.8		4.7	9
<b>Old Wetland Pool</b>																
09/99 (pore water)	16.0	7.8	0.77	228	0.36	0.33	98	30.8		1.59	0.06	1.05				8
04/02	18.3	7.2	2.98	309	0.48	0.46	439	132.0	196		0.07	5.85	7.5		23.11	9
10/02	25.5	7.9	2.42	349	0.47	0.51	407	145.8	599		0.12	4.74	20.8		4.09	9
<b>New Wetland Pool</b>																
09/99	19.6	7.1	2.41	193	0.26	0.26	418	56.2		8.87	0.12	9.46				8
04/02	17.0	7.5	2.65	311	0.49	0.47	436	128.8	692		0.08	5.90	22.5		4.99	9

**Note:** 1, Allen and Day 1935; 2, Fournier et al. 1991 and references therein; 3, Fournier et al. 1992 and references therein; 4, White et al. 1988 and references therein; 5, Sturtevant this study; 6, Fournier et al. 2002; 7, Ball et al. 2001; 8, Channing 2001; 9, Channing this study; 10, Virginia Rodrigues, personal communication, 2003. SI, silica saturation index; SI m20, model silica SI for fluid at 20 °C.

<sup>a</sup>Where possible dates are given as day/month/year or month/year.

**Table 2.** Character of Porkchop Geyser eruptions, wetland conditions, and vent-wetland water colouration.

(A)	Porkchop Geyser activity	Vent pool water colouration	
1920s	Intermittent geyser		1
1950s–1960s	Intermittent geyser	Fluctuating clear to opaque milky-blue	2
1960s	Seeping discharge (a few litres/min)		23
1970s	Infrequent geyser	No diffraction observed	2
1972	Infrequent geyser	Clear	4
1971–85	Infrequent–intermittent geyser	Fluctuating clear to opaque milky-blue	24
1985–89	Constant geyser mixed water–steam	Little standing water in vent pool	234
Sept 89	Hydrothermal explosion destroys much of vent–pool	Gelatinous (colloidal) silica masses expelled from vent	2
1989–91	Intermittent geyser 1–2 m high	“Opalescent” appearance	25
Early–mid 1990s	Intermittent geyser and gentle overflow of S rim	Fluctuating clear to opaque milky-blue	9
1994	Very active, spouting. Heavy overflow from S rim	Very opaque milky-blue	9
1994–96		Opaque milky-blue	6
May–Sept 1995	Outflow from S rim	Opaque milky-blue	7
Summer 1998	Quiescent	Clear	8
Sept–Oct 1998	Gentle overflow from S rim	Clear	8
Aug–Sept 1999	Intermittent gentle overflow from S rim	Opaque milky-blue	8
Feb 2000	Intermittent gentle overflow from S rim	Opaque milky-blue	8
Apr 2001	Heavy overflow from S rim for ca. 3 months	Change from clear to opaque milky-blue	9
April 2002	Constant diffuse discharge from S rim	Very opaque milky-white–blue. Mie scattering? 13 Particles dominantly > 0.45 µm (12)	10
July 2002	Constant but slow diffuse discharge from S rim	Opaque milky-blue–white. Rayleigh scattering? Particles dominantly < 0.45 µm (12)	10
Oct 2002	Constant but slow diffuse discharge from S rim	Opaque milky-blue–white. Rayleigh scattering? Particles dominantly < 0.45 µm (12)	10
Summer 2003	Constant and heavy discharge from S rim, 14/07 “spurting milky mud,” 16/07/03 eruption	Opaque milky-blue	11
(B)	Wetland pool conditions	Pool water colouration	
April 2001	Both pools flooded by heavy discharge from Porkchop	Opaque milky-blue	9
April 2002	Pools flooded, heavy sediment accretion ca. 2 cm between Spring 2001 and April 2002 in old pool	Very opaque milky white–blue. Mie scattering? 13 Particles dominantly > 0.45 µm (12)	10
July 2002	Pools flooded. Volume of water present reduced relative to April, Evaporation active?	Old pool opaque milky blue, New pool clear	10
Oct 2002	Pools flooded, ca. 0.5 cm sediment accretion between July and Oct. in old pool	Old pool opaque milky blue	10
Late July 2003	Heavy flow to both wetlands, fresh sediment accumulation on apron between vent and pools and within pools	Very opaque milky-white–blue. Mie scattering? Particles dominantly > 0.45 µm (12)	11
Sept 2003	Heavy flow to both wetlands, fresh sediment accumulation in pools	Opaque milky-blue	11

**Note:** 1, Allen and Day 1935; 2, Fournier et al. 1991 and references therein; 3, Fournier et al. 1992 and references therein; 4, White et al. 1988 and references therein; 5, Bryan 1995; 6, Ball et al. 2002; 7, Fournier et al. 2002; 8, Channing 2001; 9, Sturtevant this study; 10, Channing this study; 11, Virginia Rodrigues, personal communication, 2003; 12, Ohsawa et al. 2002.

(April), 28 °C (July) and 26 °C (October). Waters flowing from Porkchop Geyser to the wetland became more basic as they cooled and presumably degassed, usually rising by 0.1–0.2 units of pH to a recorded maximum of pH 8.2. Recorded

pH within the wetland was from pH 7–7.9. In the newly inundated wetland pool where water temperatures were only a few degrees above ambient (water temperature 10 °C in October 2002), pH reached 8.8.

**Fig. 2.** Porkchop Geyser, adjacent wetland and wetland sediments. (A) Photograph taken on 22/4/2002, illustrating the relative positions and sizes of Porkchop Geyser (surrounded by debris from the September 1989 geothermal explosion), the older of two adjacent geothermally influenced wetlands filled with opaque milky-blue water and the intervening sinter slope. Vegetation within the centre of the wetland comprises the hydrophytic, halophytic and alkaliphilic plants *Eleocharis rostellata* and *Triglochin maritimum*. The pool margins and areas of the sinter slope are colonized by alkali tolerant grasses. The area of water in the right foreground is at the margin of a newly flooded depression also receiving vent fluid from Porkchop Geyser. (B) Sedimentary structure within the wetland exposed in the walls of a pit excavated in the summer of 1999. Pen for scale. (C) Vent pool of Porkchop Geyser on 22/4/2002. Fluid in the vent is opaque milky-blue suggesting that it contains polymerized silica.



## Methods

### Imaging techniques

Sediment was mounted for scanning electron microscopy (SEM) on aluminium stubs with carbon adhesive pads. Samples were sputter coated with gold–palladium for ca. 2 min and examined with the secondary electron detector (SE) of a Cambridge Instruments S360 SEM at 25 keV accelerating voltage and 4–10 mm working distance. The abundance of colloidal silica particles caused severe charging problems arising from poor coating of spherical surfaces and (or) poor electrical conductivity between loose particles. This problem was most acute at low resolutions, where areas of good and bad coating quality lay in the field of view, and at the highest resolutions required to view aggregate ultrastructure. Double applications of gold–palladium reduced charging problems. Transmission electron microscopy (TEM) imaging was conducted with a JEOL JEM1210 transmission electron microscope at an accelerating voltage of 80 keV.

### Analytical techniques

Determination of the mineral phase present was conducted with a Phillips PW1710 analytical X-ray diffractometer. Bulk powders were analysed using cavity sample holders. Operating conditions were 40 keV at 20 mA using Cu K $\alpha$  radiation. Diffraction scans were made at speeds of 0.6°/min with step size 0.01° from 10°–40°2 $\theta$ . X-ray diffraction spectra were analysed with Philips PW1876 PC-Identify software. The qualitative elemental composition of TEM samples was determined using the analytical facilities of the JEOL JEM1210 TEM, fitted with an Oxford Instruments, Link System EDX (energy dispersive X-ray) spectrometer and Link ISIS analytical software. Spot analyses were conducted at an accelerating voltage of 80 keV. Water samples collected during 1998–1999 were analysed for dissolved silica, sodium, and potassium concentrations with a Varian SpectraAA 300 series spectrophotometer. Analytical precision expressed as percent relative standard deviation (%RSD) was < 0.5%RSD for Na, K, and < 1%RSD for Si. Trace-element concentrations (Li, Mg, Al,

P, Ca, Mn, Fe, Cu, Zn, As, Ba) were determined on a PerkinElmer Elan-5000 inductively coupled plasma – mass spectrometer (ICP–MS). Only calcium and lithium concentrations exceeded 1 mg/kg. Analytical precision for this method was < 3%RSD for Li, Ca and < 4%RSD for Mg. Concentrations of the elements Al, As, Ca, Cu, Fe, K, Mg, Na, Si, and Zn of water samples collected during 2002–2003 were analysed with a JY Horiba Ultima-2 inductively coupled plasma – optical emission spectrometer (ICP–OES). Only silicon, calcium, sodium, and potassium concentrations exceeded 1 mg/kg. Analytical precision was < 2%RSD for Si, Na, Mg and < 3%RSD for Ca, K. The anions fluoride, chloride, bromide, nitrate, phosphate, and sulphate were analysed on a Dionex DX-80 ion chromatograph (IC). Only fluoride, chloride and sulphate exhibited values greater than 1 mg/kg. Calculated analytical precision was < 1.5%RSD for F, Cl and < 4.5%RSD for SO<sub>4</sub>. Physical and chemical properties derived from field and laboratory water analysis were used to model indices of silica saturation (SI) using the geochemical program PHREEQC. Particle and aggregate size distributions were assessed by light scattering analysis. Bulk samples of silica sediment prepared for X-ray diffraction (XRD) analysis were also analysed for carbon, hydrogen, and nitrogen concentrations with a PerkinElmer, Series II 2400, CHN analyser.

## Results

### Mineralogy

The major mineralogical component of the silica sediment was determined to be amorphous opal-A by X-ray powder diffraction. Diffraction patterns exhibited a broad diffraction band with low maximum count intensities, centred variably on 22°–23°2θ.

CHN analyses of bulk wetland sediment revealed an extremely low-sediment carbon concentration. Values returned (0.04%–0.06%) fall at or below the detection limit of the analytical system. Sediment from a diatomaceous wetland analysed for comparative purposes in contrast contained between 0.13% (surface sediment) and 0.82% (bulk sediment) carbon.

### Sedimentary structure

Depositional sedimentary structures, sediment accretion rates, and lateral variations within the wetland were investigated by coring (Fig. 3J) and trenching (Fig. 2B) during the summers of 1998 and 1999, whilst the wetland surface was dry and exhibited desiccation cracks. Sedimentary structures, particle size, composition, morphology, and biota are summarized in Table 3.

The irregular (probably unglute bioturbated) surface horizon of the sediment contained rare partially silicified higher plant material. Discontinuous consolidated–dehydrated areas of sediment surface formed blocky, friable, bedding-parallel clasts that superficially looked like the laminated sinter more characteristic of sinter aprons. A discontinuous green horizon was apparent at variable depth just below the surface in some areas of the pits (Fig. 2B). Microbes isolated from this horizon include diatoms and microbial (probably cyanobacterial) filaments.

Parallel to wavy and cross-bedded and contorted bedding–lamination were the dominant fabrics within the upper sections

of both pits and core (Figs. 2B, 3J, horizons a–d). Bedding and lamination were visible due to sediment colour and opacity variations. Small bedding-parallel lenses, ca. 2–3 cm long and 0.5–1 cm deep, were discernible in the upper horizons of the 1999 pit (Fig. 2B).

Sediment toward the base of pits and core appeared more massive, the marked changes in sediment colour and sediment structure of the upper horizons being replaced by subtle mottling and poorly defined bedding (Fig. 2B). Poorly discernible laminations marked by changes in sediment colour from opaque white to opaque green-grey (Fig. 3J, horizon f) corresponded to sequences of upward fining particle size. A soil–exposure horizon, developed ca. 13–15 cm below the sediment surface (Fig. 3J, top of horizon f), contained grass stems and rootlets. Below the soil horizon were ca. 10 cm of mottled, opaque white to grey sediment. Traceable laminations within this horizon fluctuated in depth below the sediment surface by several centimetres across the width of the trial pits and the core. The oldest sediments comprised grey-brown clay-like matrix with detrital sinter and volcanoclastic clasts (Fig. 3J, horizons g–i). The base, both of cored sediment and pits, coincided with a layer of sinter clasts in a clay to mud-like matrix, which was impenetrable using the core pipe.

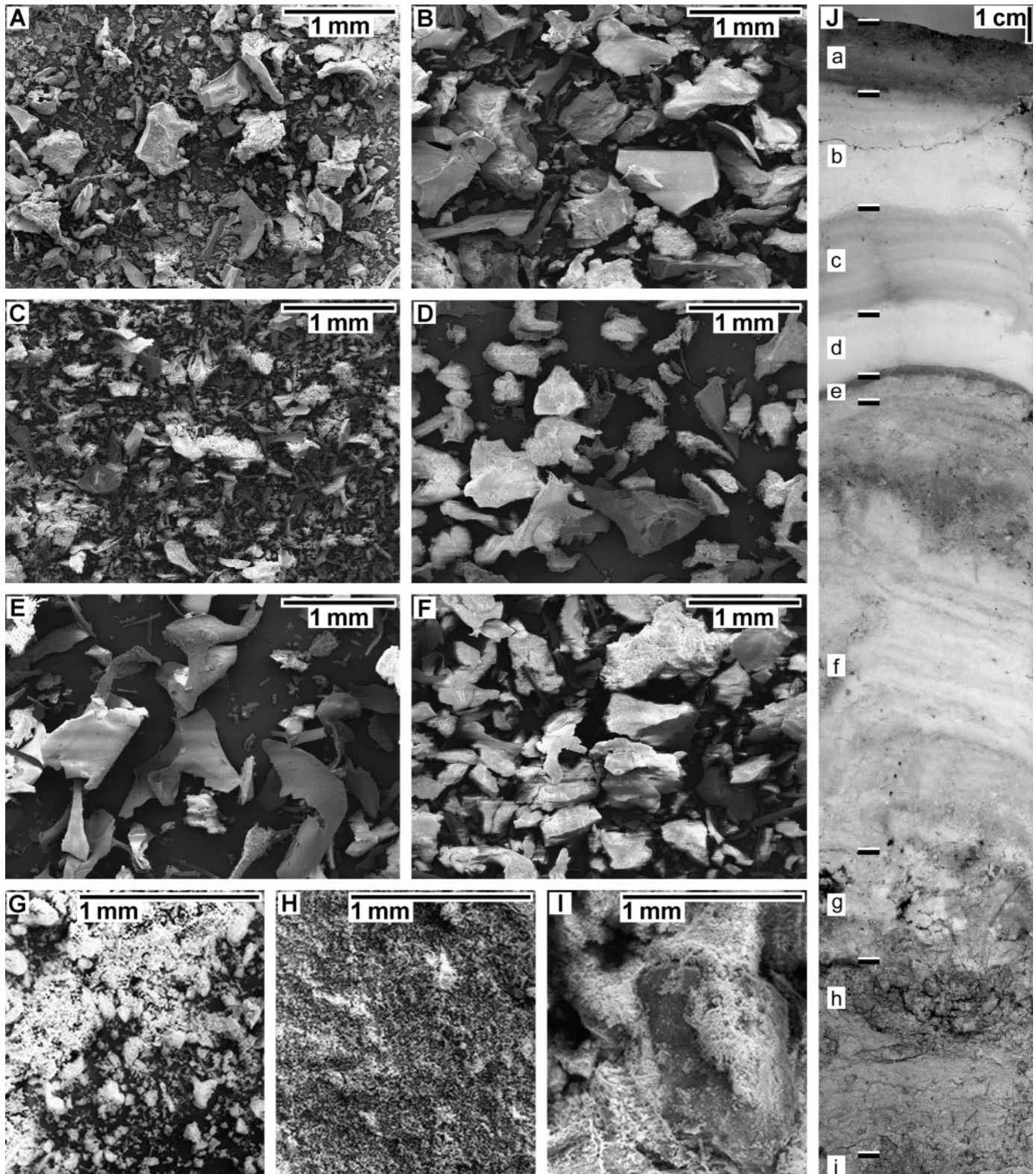
### Active wetland sedimentation

During the active period of wetland flooding observed between April 2001 and October 2002, sediment accumulation formed a massive white sediment horizon ca. 2–3 cm thick (Figs. 4A–4C) that extended across the entire wetland surface. Sediment engulfed wetland plants, commonly the halophytes *Triglochin maritimum* and *Eleocharis rostellata* and alkali tolerant grasses, rooted in the 1998–1999 sediment surface. Growth of some of the current growing season's aerial stems and leaves occurred through freshly deposited silica (Fig. 4C). At the pool margin, exposure and desiccation created an indurated upper sediment surface with beige to brown colouration. Brecciated sinter associated with the pool-margin sinter slope was becoming cemented by sediment deposition and desiccation (Fig. 4E). Stems and leaves of grasses in the same environment had collapsed to form a prostrate radial pattern. Organic surfaces were coated with robust layers of indurated silica sediment (Fig. 4D). Desiccated sediment that adhered to the sinter apron surface appeared massive, dull and grainy relative to true sinter apron surfaces.

### Particle morphology

Scanning electron microscopy (Figs. 3A–3I) assessed particle size, size variation, morphology, and composition from nine horizons within the core (Fig. 3J, horizons a–i). Mineralogy of each horizon was assessed by XRD. Particle size distribution of sample horizon f was analysed further by light scattering techniques and transmission microscopy. The qualitative trace-element composition of the same material was investigated by electron probe X-ray microanalysis (EPXMA). The sediment was dominated by particles considered to be of chemically precipitated origin (particle types 1–3 described in the following subsections). Biochemically precipitated silica particles, diatoms (particle type 4) were less common in the bulk of the sediment but were important constituents within individual horizons (Figs. 5A–5D).

**Fig. 3** (A–I) SEM images illustrating typical clast size and morphology of nine sediment horizons of the wetland (Fig. 3J, horizons a–i, respectively). (J) Core sample of the wetland sediment. The domed appearance of sediment in the core is in part due to deformation associated with core manufacture.



**Type 1 particles: silica microspheres**

The simplest particles observed within the wetland sediment were silica spheres (microspheres) with nanometre to micro-

metre dimensions. Microspheres of ca. 10 nm to ca. 1  $\mu$ m were observed to form particle aggregates described in the next subsection. Less common isolate silica microspheres,

**Table 3.** Wetland-sediment structure, mineralogy, and biota.

A	(A) Irregular surface, beige-brown. Organic clasts, charcoal, and partially silicified plants. Often partially lithified. Translucent grey below surface. Discontinuous green horizon, diatoms, filamentous microbes. Opal-A.
B	(B) Sediment cleaner, white-beige. Diffuse bedding–laminations above, more massive to base. High percentage of dense glassy (type 3) clasts between ca. 100–500 $\mu\text{m}$ . Opal-A. Sparse diatoms.
C	(C) Translucent–opaque grey, white bedding–laminations to 0.5 cm thick. Sediment lenses and cross-bedding above, parallel beds at base. Large quantities of smaller and (or) floc-like type 2 clasts up to ca. 500 $\mu\text{m}$ . Opal-A. Diatoms not observed.
D	(D) Massive opaque white horizon ca. 2 cm thick. Diffuse upper boundary. Glassy shard-like (type 3) particles ca. 100–200 $\mu\text{m}$ . Opal-A. Diatoms not observed.
E	(E) Sharp boundary between 3 mm-thick translucent-grey horizon and massive white horizon above. Horizon E, high percentage of dense glassy (type 3) clasts between ca. 100–500 $\mu\text{m}$ . Opal-A. Sparse diatoms.
F	(F) Top of F soil–exposure horizon, variable thickness brown-beige colouration. Plant stems, organic/charcoal clasts. Opal-A. Sparse diatoms. Below, mottled and (or) contorted bedding. Colour variations from opaque-white to opaque-grey–green. Colour changes correspond to upward fining clast size sequences. Laminations fluctuate in depth below sediment surface by several centimetres. Wide variation in clast size. Upper limit of clast size occurs in opaque grey material reaching ca. 1 mm. Floc-like type 2 particles occur in whiter opaque material. Opal-A. Diatoms initially sparse but becoming more abundant to base.
G	(G,H,I) Beige-brown matrix, increasingly clay-rich with diatoms becoming much more abundant to base, representing ca. 50% or more of the sediment. Lithic clasts of volcanoclastic–geothermal origin. Clast size increases and clasts become more angular to base. Horizon H Diatomaceous. Opal-A plus smaller quantities of kaolinite, quartz, and cristobalite.
H	
I	

Note: Sediment horizons A–I correlate to horizons a–i of Fig. 3J.

with diameters up to 10  $\mu\text{m}$  (Fig. 5E), occurred in horizons in association with all three major particle types.

#### **Type 2 particles: open floc-like silica microsphere aggregates**

Open floc-like aggregates, with a low degree of particle coalescence caused extreme charging and flaring when the particles were observed with SEM (bright areas of large flocs Figs. 3C and 6A). The larger flocs in horizon c reached ca. 500  $\mu\text{m}$  diameter, but the primary aggregates into which they readily broke down were of submicron dimensions. Light scattering techniques indicated that the primary aggregates within the sample had a unimodal size distribution of ca. 200 nm. TEM observation showed that the size distribution reflected primary aggregate size and distribution (Fig. 6B). The smallest units of the primary aggregates were type 1 silica microspheres ca. 10 nm in diameter (Fig. 6C). The disordered nature of the contact points between primary particles and primary aggregates dictated that the larger flocs had a disordered morphology. EPXMA spectroscopy of the primary aggregates indicated the presence of Na, Mg, Al, P, S, Cl, K, and Ca in addition to much higher levels of Si, O, and C (Fig. 6D).

#### **Type 3 particles: dense silica microsphere aggregates**

The most common aggregated particle morphology throughout the core comprised dense, glassy, often shard-like silica particles. When observed with a light microscope, these appeared either glassy and clear or more opaque and beige-brown (Figs. 7A, 7B), depending on the thickness of silica and orientation of the surface in the area viewed. Brown colouration appeared to derive from light scattering effects created by the dense, though partially open, particle network. SEM photomicrographs reveal a structure comprising variably sized silica particles in a disordered aggregate with a high degree of coalescence and little interparticle porosity (Figs. 7C, 7D).

#### **Type 4 particles: diatom bioclasts**

Diatoms, abundant eunotioid (Fig. 5C), and anomoeoneid genera and species were present at the base of the core (Fig. 5D). Naviculoid (Fig. 5A) and achnanthoid (Fig. 5B) genera were present in low numbers throughout the upper horizons of the core, with the exception of horizons c and d (Fig. 3J). Abundance increased considerably toward the base of the core. Diatom frustules contributed ca. 50% or more of the sediment (Fig. 5D) of horizons g, h, and i (Fig. 3J).

#### **Other clasts**

XRD analysis of horizon h (Fig. 3J) indicated the presence of smaller quantities of kaolinite, quartz and cristobalite, probably resulting from clastic sedimentation of underlying hydrothermally altered kame and (or) volcanoclastic materials. Clasts of opal-A sinter were common towards the base of the core and trial pits.

#### **Particle type distribution and size variation**

Differences in sediment colour and opacity between sediment horizons corresponded to systematic particle size–morphology and colour–opacity associations. Horizons within the core with an opaque colouration (Fig. 3J, horizon b, e) generally contain a high percentage of dense glassy particles between ca. 100 and 500  $\mu\text{m}$  diameter (Figs. 3B, 3E), whilst translucent grey horizons (Fig. 3J, horizon c) contain greater quantities of smaller and (or) large but extremely delicate floc-like particles (Fig. 3C).

## **Discussion**

### **Sedimentary structure**

The trial pits revealed the lateral continuity of the major lithological units and discontinuities visible in the core, suggesting periodic basin-wide changes in the geochemical

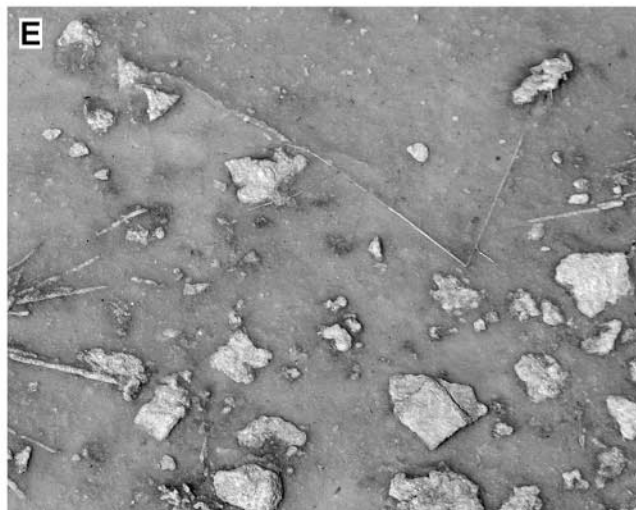
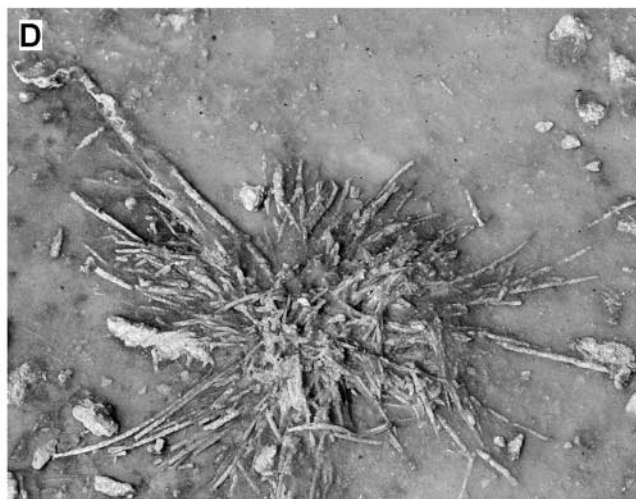


**Fig. 4.** Active wetland sediment accretion and plant–sediment interaction. (A) Fresh, white silica sediment deposited on the wetland surface between April 2001 and October 2002. Leaves and stems of *Triglochin maritimum* have grown up through the sediment. Depressions in foreground are ungulate hoof-prints. (B) Depth of fresh sediment horizon revealed by hoof-print. (C) Partially dehydrated–consolidated sediment horizon at pool margin being fractured and lifted as a slab by the growth of *Triglochin maritimum*. (D) Leaves and aerial stem of a grass on the slope between Porkchop and the wetland. Sediment covering the plant has become dehydrated, consolidated, and resistant to remobilization. The plant illustrates a radial pattern typical of organs that have fallen at the end of a growing season or been killed by immersion in spring waters. (E) Sinter chips one slope between Porkchop Geyser and wetland partially buried and “cemented” to apron surface by sediment accumulation and dehydration.

and (or) sedimentological regime. These most likely reflect changes in the discharge regime and (or) water chemistry of Porkchop Geyser. The sediment sequence described in the previous section appears to show the creation of a basin within an area relatively unaffected by geothermal activity, but with aquatic or damp conditions indicated by the presence of diatoms in the basal sediments (Figs. 5A–5D). Clays and silica clasts in the basal sediments (Figs. 3G–3I) suggest that initially sedimentation was dominated by influxes of material derived from weathering of older sinter sheets, altered volcanoclastic material, and kame surrounding the wetland. Alternatively the sediments may be detrital sintraclasts and ejecta (following the terminology of Jones and Renaut 2003) derived from the vent apron of Porkchop Geyser. The basin may have dissected the local water table, but more likely, acted as a perched basin due to the presence of silica-cemented basement rocks (White et al. 1988) or the initial lining of clay-rich material.

Initially, the basin was colonized extensively by diatoms, e.g., *Eunotia* sp., diagnostic of relatively low pH, low dissolved mineral content, and fluid temperatures between ca. 15 and 25–30 °C (e.g., Vinson and Rushforth 1989). Progressively, the basin became influenced by geothermal fluid input and, as diatom species diversity declines at temperatures above ca. 25–30 °C (e.g., Vinson and Rushforth 1989 and references therein), diatom numbers and diversity waned (Fig. 3F). Achnantheid and naviculoid diatoms present higher in the sediment (e.g., from Fig. 3J, horizon f) suggest an associated increase of wetland pH. Chemical precipitates began to form the major sediment component. Sediment accretion was relatively constant and changes in sediment deposition rates and sediment character small. Fining-up sequences of particle deposition indicate periodic sediment influxes or fluid influxes and associated polymerization and precipitation sequences. There is no evidence for desiccation events until the major organic horizon (Fig. 3J, top of horizon f) 10–15 cm above the base of the section.

Following colonization of the pool by grasses, conditions again returned to sediment accretion. The presence of unbleached and poorly silica encrusted plant material above the soil horizon indicate that initial burial of the exposure surface was rapid. The resumption of deposition was most likely accompanied with waterlogged soil or aquatic pool conditions, which may have restricted oxidative and microbial decay of organic material incorporated within the sediment profile. Strongly bedded and laminated horizons (Fig. 3J, horizons e–b), with marked changes in sediment particle-size and morphology, indicate strong temporal variations in the water table, sediment and (or) silica supply, and mechanism of particle formation prior to drying of the basin and formation of the surface soil horizon (Fig. 3J, horizon a) apparent from

ca. 1998–2001. The dominance of parallel and undulating bedding and laminations suggest periods of precipitation and (or) sedimentation from a pool of standing water. During the latter stages of sediment accretion periodic influxes of water created cross-bedded horizons (Fig. 2B), either as material new to the basin was deposited from the fluid or as existing sediment was remobilized. Deformation fabrics may have resulted from a number of phenomena. Trampling by large mammals has occurred in the recent past as evidenced by hoof prints (Figs. 4A, 4B). However, dewatering, cryoturbation, seismicity and explosive hydrothermal activity may also have played a role in deformation.

#### Particle formation

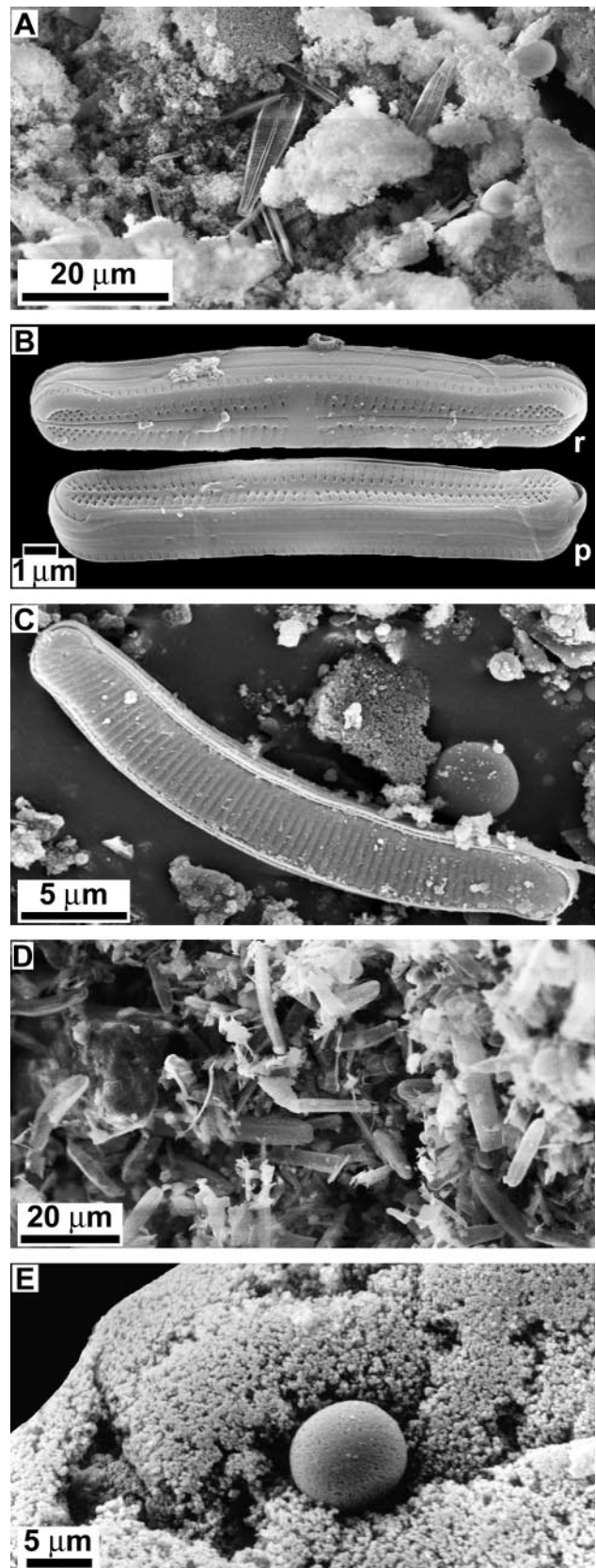
The paucity of carbon within bulk sediments from the basin relative to sediments collected from wetlands dominated by diatomite accumulation is here considered a reflection of the essentially abiotic nature of the majority of the sediments discussed in the following subsections. The presence of C, P, S, Na, Ca, Mg, Cl, and K, all biologically important elements, in EPXMA spectra of silica particle aggregates could be regarded as evidence for mediation of particle aggregation by dissolved or suspended organic molecules and (or) substrates, such as the extracellular polymeric substances (EPS) of diatoms or bacteria. The same elements are also found dissolved in hot spring waters where they derive from water–rock interactions. K, Na, Cl, Ca, and Mg, as discussed below, are implicated in colloidal aggregation and precipitation of silica. The ultrastructure of type 2 and 3 particles supports their formation through chemical rather than biochemically mediated processes. The particles lack any evidence of either morphological or organic microfossils, but most obviously they have a particle aggregate structure constructed from submicron type 1 silica microspheres that indicate formation through colloidal activity (compare Fig. 6B with Everett 1994 fig. 9.8 or Iler 1979 figs. 5.20a, 5.20b).

#### Type 1 particles

Following silica nucleation, polymerization increases the radius of silica particles (microspheres) until they reach colloidal dimensions and create a particle dispersion (sol). The range of particle sizes observed in type 2 and 3 particles (between ca. 10 nm and 1 µm) fall within the limit of colloidal dimensions (e.g., Iler 1979; Bergna 1994; Everett 1994, p. 5). Sols may be destroyed by the growth of individual particles to dimensions beyond ca. 1 µm, at which point colloidal forces cannot prevent their sedimentation (e.g., Iler 1979; Bergna 1994; Everett 1994).

Large individual silica spheres were a relatively rare occurrence within the sediment. However, particles of 1–10 µm diameter were observed. Their growth is possible by two

**Fig. 5.** Scanning electron photomicrographs. (A) Diatomaceous and floc-rich sediment from Fig. 3J horizon f. (B) *Achnanthisdium* sp.: r, raphe valve; p, pseudoraphe valve. (C) *Eunotia* sp. (D) Diatomaceous sediment from horizon i (Fig. 3J) dominated by type 4 particles, diatom frustules, including the genera *Anomoeoneis* and *Eunotia*. (E) Large type 1 silica particle, indicative of prolonged periods of particle growth and sol stability, resting on a larger dense but partially open, aggregate particle.



mechanisms. In low-energy conditions (as are envisaged at most times in the wetland pool), high pH and an absence of dissolved salts could have created strong interparticle repulsion and maintained sol stability allowing continued particle growth. In higher energy conditions (e.g., the vent fluid of Porkchop Geyser), turbulence could discourage interparticle collisions and adhesion and particle settling and have a similar effect.

#### *Type 2 particles*

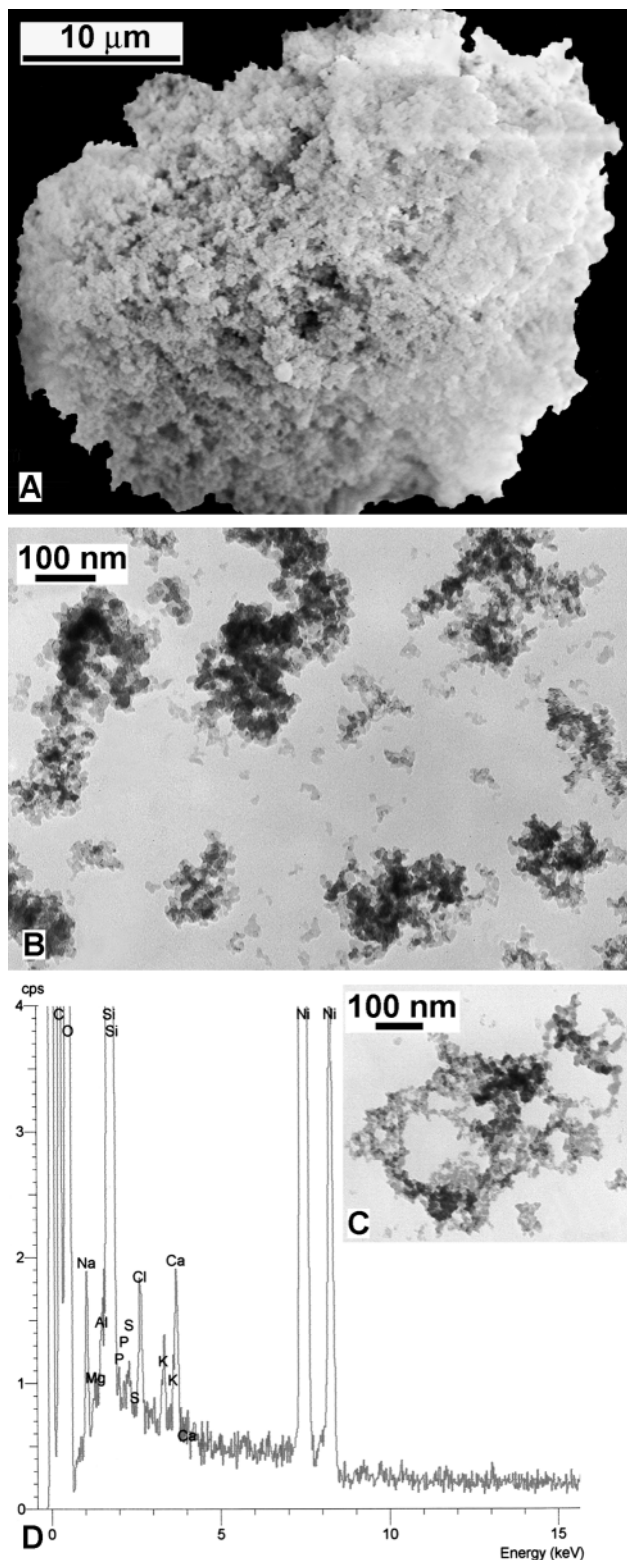
The dimensions of primary particles and primary particle aggregates of type 2 particles (10 nm and 200 nm, respectively) are well below the upper dimensions of the colloidal range. Aggregation phenomena, such as coagulation, gelation, or flocculation, must have been active for the particles to have precipitated from solution. The characteristic open structure, low degree of particle coalescence, disordered distribution of contact points between primary particles, and susceptibility of the particles to disintegration appear to suggest that the type 2 particles were formed by flocculation. Flocculation creates open particle aggregates by reducing interparticle repulsion in the sol. Flocs may or may not separate out of suspension (precipitate). Flocculation may be achieved by lowering pH from alkaline to neutral or acid and thus removing repulsive forces between particles, cation-bridging, especially if concentrations of cations were high, or the introduction of positively charged colloids (e.g., Iler 1979; Bergna 1994; Everett 1994). The large voluminous and open floc-like type 2 particles of sediment horizon c (Fig. 3J) appear comparable to particles flocculated during rapid diffusion-limited aggregation (Lin et al. 1989). The disordered primary particle distribution observed by TEM (Figs. 6B, 6C) illustrates flocculation of weakly repelling to strongly attracting particles that on contact have become fixed in the configuration in which they collided (e.g., Everett 1994, fig. 9.8).

#### *Type 3 particles*

Dense particle aggregates could have formed both by colloidal and physical mechanisms. The structure of particle aggregates is strongly influenced by the interparticle forces acting within a sol. The residual negative surface charge created by hydroxyl ions at the particle surface of silica colloids makes them strongly repelling at neutral to alkali pH and low salt concentrations. In these conditions aggregation by coagulation can create dense particle aggregates as particles collide and, instead of becoming attached to adjacent particles in their collision configuration, slide across one another under the influence of Brownian motion and pack in a configuration of minimum energy (Everett 1994). Following aggregation in a dilute sol (where the volume of aggregate particles relative

to fluid is low) the dense aggregate particles precipitate from suspension.

Dense coagulum-like particles may also have formed by



the destruction of a sol via a gel-phase. Gelation creates a coherent three-dimensional network of particles that may become viscous, and solidify and fill the entire volume of the sol (e.g., Iler 1979; Bergna 1994). In hot conditions, evaporation of a sol may form a gel-like film as the colloidal particles are compressed by the surface tension of enclosing water as it is drawn down. Continued dehydration causes

**Fig. 6.** Type 2 open flocc-like particle aggregates. (A) Scanning electron photomicrograph of large open flocc-like particle isolated from wetland core (Fig. 3J, horizon f). The poorly coalesced–cemented nature of particles that make up the large particle cause charging and flaring, as gold coating of the particle network is incomplete. Disintegration of particle aggregates under the SEM electron beam creates further uncoated surfaces. (B, C) Transmission electron photomicrographs illustrating typical morphology and ultrastructure of open flocc-like particles. Particles comprise type 1 silica microspheres of ca. 10 nm diameter, have a disordered relatively open flocc-like structure, exhibit a low degree of particle coalescence and poor structural stability. Light scattering techniques (data not illustrated) suggest that large type 2 particles readily broke down into smaller primary particle aggregates of ca. 200 nm diameter. (D) Electron probe X-ray microanalysis (EPXMA) spectra, providing qualitative trace element composition of silica particles from Porkchop wetland. cps, counts per second.

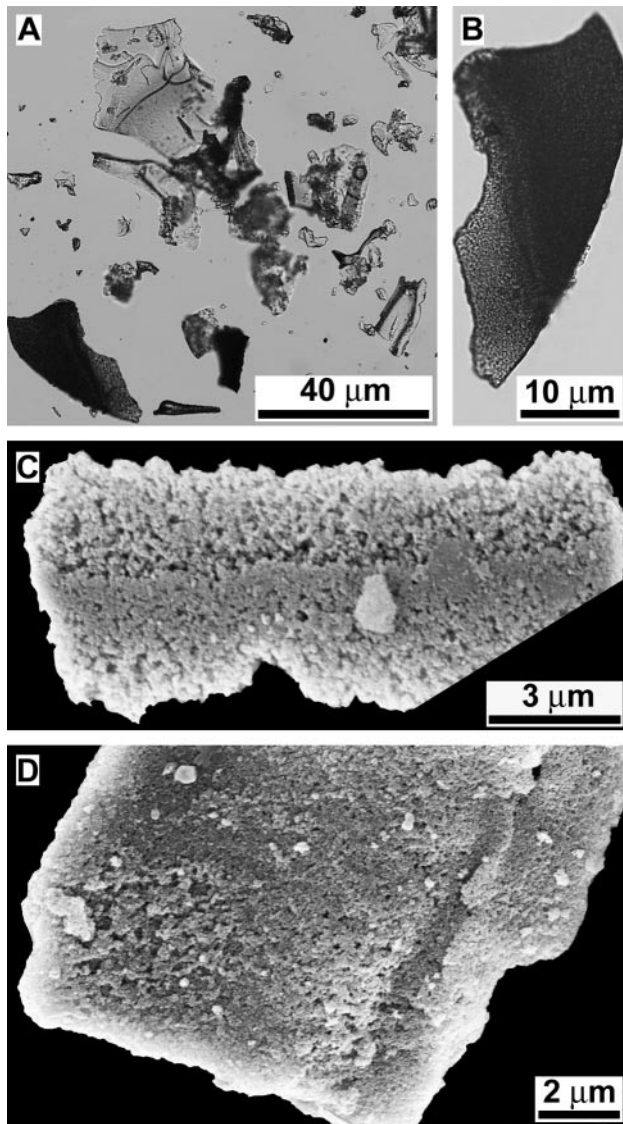
fracturing of the gel by shrinkage and creates relatively dense fractured silica aggregates (e.g., Iler 1979, fig. 4.15). The fractured surface morphology of many type 3 particles may imply that, during some periods, this evaporative mode of formation was active. Gelation is also possible via rapid freezing of a sol (e.g., Bergna 1994). As discussed further later in the text, this mechanism may be particularly important in Yellowstone where geothermal waters issue from hot springs into a winter environment characterized by sub-zero temperatures.

The structure of silica particle aggregates is most easily observed when the particles are suspended or freshly precipitated from a dilute sol (Iler 1979; Bergna 1994). However particles observed in this study were collected from wetland sediment. It is possible that some dense type 3 particles may also have formed by restructuring of more open (type 2) particles. The low structural strength exhibited by type 2 particles make them inherently unstable in environments where they are not suspended in a fluid medium, for instance following sedimentation and sediment accretion, where increasing pressure is exerted by overlying sediment. Weakly bonded flocs may also be compressed in a manner described earlier in evaporative gel formation. Open flocc-like particles may become denser and more indurated as further silica is precipitated onto silica particle surfaces. This requires that the environment in which the flocs are deposited retains silica at concentrations above saturation but with a low enough degree of saturation to prevent fresh particle nucleation.

#### Mechanisms of sediment–wetland formation

Fluids flowing into the wetland (and therefore either directly or indirectly the sediments at present accumulating on the wetland surface) undoubtedly derive from the vent pool of Porkchop Geyser. The topography of the area suggests that sediments deposited prior to 1998 accumulated from the same source. Three locations of particle formation are clearly possible; the Porkchop Geyser vent system and vent pool, the sinter apron, and the wetland. One or all of these environments may have been active during the history of sediment accumulation. The presence within the wetland of three distinct colloidal particle morphotypes and a record of variable

**Fig. 7.** Type 3 dense, glassy, shard-like particle aggregates. (A, B) Light photomicrographs illustrating typical morphology and glassy, shard-like character of type 3 particles. Beige-brown colouration probably derives from light scattering in the dense though partially open aggregate structure. (C, D) Scanning electron photomicrographs illustrating ultrastructure of type 3 particles. Particles exhibit a high degree of particle coalescence but retention of interparticle spaces. Highly variable particle size and degree of particle coalescence within aggregates creates a fabric similar to potch-opal.



sediment accumulation suggests changeable conditions of particle precipitation, deposition, and (or) provenance.

The relative abundance of particle morphologies in the geothermal wetland differs substantially from those observed in diatomaceous wetlands. Diatoms formed only a minor component of the sediment within horizons above the basal breccia and clayey diatomites, suggesting conditions hostile to their growth. Large clasts of volcanoclastic and sinter material were also scarce above the basal horizon, suggesting the limited input of material from areas around the basin

margin other than Porkchop Geyser. Chemically derived particles were dominant throughout the upper ca. 30 cm of the core. This may have been a result of slow chemical sediment accumulation over large time periods and a relative absence of diatoms. The rapid burial of soil horizons and sediment accumulation rates observed between April 2001 and October 2002, however appear to indicate accumulation was more likely a result of rapid silica polymerization and (or) sedimentation.

Here we discuss two potential mechanisms that may be implicated, either individually or collectively, in the creation of the Porkchop Geyser wetland sediments.

- (1) The wetland forms an ephemeral pool that received fluid from Porkchop Geyser containing colloidal silica particles and dissolved silica. Colloidal silica nucleates and polymerizes in high-temperature regions of the system and is transported as solid particles and aggregates to the wetland. Wetland waters containing silica concentrations above saturation locally polymerize silica either to existing colloidal particles–precipitate or potentially nucleate fresh colloids.
- (2) Gelation produces particulate silica during freezing of geothermal waters during the Yellowstone winter. Particulate is formed on the sinter apron and is transported later to the wetland depression.

#### *Ephemeral pool: deposition of silica directly from vent fluid*

From April 2001 until at least October 2002 the wetland acted as a catchment basin for fluids that constantly discharged from the vent pool of Porkchop Geyser. The desiccating conditions experienced in the same area between summer 1998 and February 2000 indicate the ephemeral nature of the pool. Porkchop Geyser has historically maintained high concentrations of silica, calculations of saturation indices show silica saturation or supersaturation of all available water analyses (Table 1). Model saturation indices for vent fluid cooled to 20 °C (SI = 0.60–0.83) indicate that erupted fluid would attain high degrees of silica saturation, which favour homogeneous silica nucleation and polymerization and promote colloidal particle growth (e.g., Iler 1979; Fournier 1985). Both analytical data (Fournier et al. 1991) and anecdotal observations of an opalescent milky-blue colouration suggest that vent fluids commonly contained polymerized and colloidal silica (Ohsawa et al. 2002). Fluid erupted from the vent at such times would, providing particles were not deposited on the intervening sinter apron, carry colloidal particles to the wetland. Sediments in the wetland therefore, may simply have accumulated as erupted fluid flowed into the basin, and suspended particles and particle aggregates precipitated in the calm wetland conditions. Large isolate silica microspheres, a common component of unconsolidated silica sediments accumulating in vent pools (Braunstein and Lowe 2001; Jones and Renaut 2003; Lowe and Braunstein 2003), may be evidence that such particles formed under turbid fluid conditions in the vent pool, and then were transported to the wetland. The constant diffuse outflow of vent fluid observed during the period of sediment accretion may aid suspended colloid and particulate transfer to wetland areas by preventing accretion to apron surfaces as it maintains turbulence and discourages

sol destruction by the formation of gels via evaporative removal of the liquid phase.

***Ephemeral pool: in situ polymerization and colloidal particle and aggregate formation***

The presence, in the wetland, of fluids supersaturated with respect to silica ( $SI = 0.26\text{--}0.51$ ) and with an opalescent colouration indicates that both silica polymerization and colloidal activity are likely to continue following the arrival of erupted water in the wetland. Measured silica concentrations at the vent pool outflow (329 mg/kg) and within the wetland pools (309–311 mg/kg) during April 2002 illustrate that the short distance between Porkchop Geyser's vent and constant water flow also favour relatively high percentages of dissolved silica in vent fluid remaining in solution during transit to the wetland. The discharge flow rates were clearly sufficiently high and the residence time of water on the sinter apron (and hence the degree of cooling) sufficiently low that little silica polymerization occurred. Additionally, the pH increases associated with vent fluid cooling and  $\text{CO}_2$  release following eruption mean that colloidal particles polymerized either in the vent or during fluid flow to the wetland would be increasingly repelled from one another also promoting continued dispersion. Once in the wetland, however, particles of colloidal dimensions would be subjected to colloidal processes dictated by the prevailing physicochemical conditions, these would derive in part from the water already in the basin plus in-flowing water.

Following eruption, fluid temperature would rapidly drop (e.g., 68.2–18.3 °C in April 2002), forcing increased silica supersaturation (from  $SI = 0.14$  at the vent pool outflow to  $SI = 0.46\text{--}0.49$  in the wetlands) and perhaps promoting homogeneous nucleation (Fournier 1985) or nucleation to the surfaces of any metal hydroxides present (Williams and Crerar 1985). However, polymerization to previously nucleated colloidal particles (Hinman and Lindstrom 1996) that may have been abundant in the fluid, as evidenced by vent fluid colouration, may stifle fresh nucleation events.

The opalescent milky-blue colouration of standing water in the wetland during 2001–2003 (Fig. 2A) illustrates that silica was present as suspended colloidal particles and (or) floc-like precipitate throughout this period. The relatively calm waters of the wetland appear unlikely to maintain particle suspension due to turbulence, chemical conditions conducive to sol formation, and sol stability may thus be deduced. Pool pH must have remained relatively high to promote particle repulsion and salinity and cation concentrations remained low enough to prevent flocculation. However, sediment did accrete to the wetland surface during this period that contained predominantly shard-like type 3 particles. The wetland was flooded at all times of observation. Gelation of colloidal silica via an evaporative route was not therefore active. By elimination, fresh sediment was forming, if type 3 particles represent a primary particle morphology (rather than a secondary morphology created by collapse of, or later silica deposition onto, floc-like type 2 particles) dominantly via coagulation.

At the pH (7.0–7.9) prevalent in the wetland during spring–summer 2002, colloidal silica particles would be strongly repelling and preferentially remain suspended as a sol. Coagulum-like precipitates could form via two apparent

mechanisms. Particles, entrained in vent fluid entering the wetland, that were of dimensions beyond the range of colloidal stability for the pool, would rapidly sediment out forming a layer of precipitate. Particles in the colloidal range would be repelled from one another and could grow by the addition of dissolved silica. On reaching the upper limit of colloidal stability for the environment, these would also precipitate and add to the forming silica layer. Restructuring of the sediment by compaction through loading could create a dense, close-packed sediment.

The continual presence of standing water in the wetland during 2001–2002 militates against the formation of dense silica particles by gelation induced by phases of evaporation. However, the process may have been active during other phases of the pool's history, for instance, prior to the development of the two soil horizons colonized by grasses. A change in the eruption frequency of Porkchop Geyser could stop or reduce replenishment of fluids in the wetland leading to evaporative draw-down of standing water. Evaporation would increase silica concentration, driving the fluid towards, or increasing the degree of, silica supersaturation. At the same time, this would reduce the volume of fluid relative to the colloidal fraction. These phenomena would promote colloidal particle aggregation, either by increasing the number of particles per volume of sol, by encouraging particle nucleation, or by increasing interparticle collisions (e.g., Iler 1979). However, evaporative concentration of dissolved components would also increase the concentration of simple salts and polyvalent cations in the fluid promoting flocculation. Either a gel or concentrated film of silica flocs would, therefore, most likely result from complete evaporative draw-down. Wetland sediment pore water contained dissolved silica at a supersaturated concentration ( $SI = 0.36$ ) of 220 mg/kg during the summer of 1998. Deposition of silica from this fluid could be implicated in infilling void space in a gel-like layer increasing particle density, whilst continued desiccation of a particle sediment could provide a potential mechanism leading to fracturing of gel-like horizons.

Colloidal particles suspended in a sol have, in the wetlands past, been subjected to rapid flocculation as evidenced by horizons in the core dominated by type 2 floc-like particles. Flocculation could be induced in the pool by a rapid reduction of pH (e.g., Iler 1979), perhaps brought about by an influx of rainwater–meltwater (at pH ca. 5.6) or a change in the hydrochemistry of Porkchop Geyser. Influxes of rainwater or meltwater would increase the volume of fluid relative to colloidal particles and reduce silica concentration, potentially decreasing the number of interparticle collisions and halting silica polymerization. Flocculation could also be induced by the addition of flocculents. These could be biomolecules such as bacterial or diatom EPA (e.g., Guidry and Chafetz 2003a, 2003b and references therein) or metal hydroxides (e.g., Williams and Crerar 1985) introduced by a change in vent hydrochemistry. Influxes of Na, K, Ca, Mg, and Al, all detected in type 2 particle aggregates during EPXMA analysis, and K, Na, Ca, and Li amongst others detected by atomic absorption spectrometry (AAS) and ICP–MS analysis of Porkchop's vent fluid and wetland sediment pore water offer potential flocculation triggers.

A rapid change in pool pH provides a simple mechanism capable of creating graded sediments of dense to open

particles. An influx of low pH fluid reduces the repulsive forces maintaining the suspension of relatively dense particles, which sediment rapidly. At the same time, repulsion between smaller colloids is reduced and large but voluminous open-flocs aggregate during a period of rapid diffusion-limited aggregation. As they have slow settling rates relative to denser particles, they initially remain suspended and slowly settle out. Flocculation gradually depletes colloids in the sol reducing particle–particle collisions, floc creation slows and compact flocs characteristic of rate limited aggregation form and settle out.

### *Cold climate processes*

Average air temperatures on the Yellowstone Plateau remain below freezing from November to April each winter. Average minimum monthly temperatures for 1971–2000 were below zero for all months, except June to August (<http://www.wrcc.sage.dri.edu>). Thus, geothermal fluids erupted from hot springs and geysers during these periods are potentially subjected to extremely rapid cooling. In the coldest months, erupted water may freeze only centimetres to metres from the vent pool. This freezing has a dramatic effect on silica precipitation. Fluid containing polymerized and colloidal silica particles in a dilute sol undergoes a natural process analogous to the industrial process of cryogelling (Bergna 1994). Silica particles in the fluid are physically forced together at ice crystallization fronts and form a dense gel as they are concentrated at the interstices of adjacent crystals. This forms solid silica precipitate that forms mobile sediment on melting of the ice. Sediment formed in this manner may be trapped on sinter aprons in or below ice for the duration of the winter. The onset of thaw conditions in spring liberates particulate silica. Sinter aprons associated with many silica-depositing springs of Yellowstone are characterized during the early spring months by relatively extensive deposits of silica sediment that may reach depths of tens of millimetres (Fig. 8A).

The common presence of colloidal silica in the vent waters of Porkchop Geyser and often continuous, diffuse outflow from the vent make gel formation via freezing a likely process of silica precipitation around the feature's vent pool. Fresh, unconsolidated silica sediments were observed forming or trapped below ice in the area immediately adjacent to Porkchop's vent during February 2000 (Fig. 8B). Similar sediments were apparent extending from the vent pool, across the sinter apron and into the wetland in April 2002.

During the period in which Porkchop continuously erupted as a geyser, spray formed an ice cone each winter adjacent to the vent pool. Anecdotal evidence suggests that the ice cone grew to a height of ca. 2.5 m and that the ice was "draped in translucent silica gel" (Schreier 1999, p. 30). Although ice cones had not formed in the geyser basins visited during February 2000, areas of boardwalk that were within the spray zone of several geysers had accumulated a considerable thickness of water-ice of geothermal origin, e.g., Sawmill Geyser, Upper Geyser Basin. Here, insulated from the thermal ground, water-ice several tens of centimetres thick had accumulated (Fig. 8C). Clumps of opaque silica particles up to ca. 2 cm diameter (Fig. 8D) were distributed randomly throughout the ice matrix forming a major component (estimated 10%–20%) of the deposit. Areas of the boardwalk where ice had melted were covered in

unconsolidated silica sediments, comparable with those accumulating on sinter sheets. Whilst some of the shard-like (type 3) particles in the wetland are likely to have formed via this process, floc-like particles require formation in a liquid medium.

### **Conclusions**

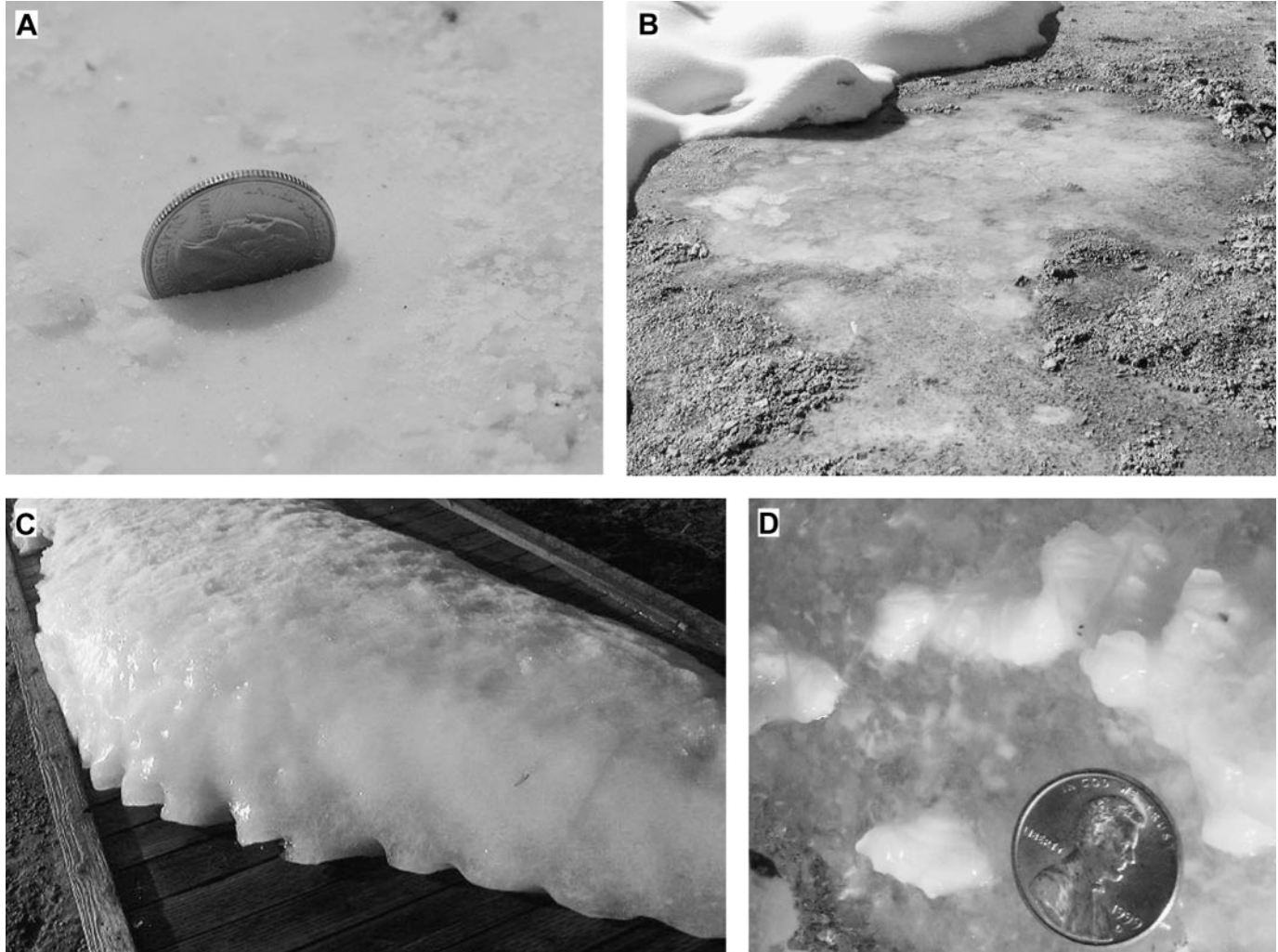
Discerning the relative importance of the mechanisms discussed in the text to sediment accretion within the wetlands is problematic. The small area of sinter apron available for sediment accumulation and low volume of unconsolidated material visible in both the summer and winter imply that, in discharge conditions comparable with those of the present day, this source would produce only minor additions to the wetland sediment, certainly volumetrically too small to produce laminae–beds of sediment millimetres to centimetres thick. Cold climate precipitation undoubtedly does generate sediment that is transported to the wetland, but again the volume appears too small to generate the observed sedimentary structures. Here, therefore, we conclude that sediment precipitation is dominantly from geothermal water collected within the wetland. Ultrastructure of the typical particles within the wetland indicates that geochemical, and specifically colloidal processes, rather than biochemical processes dominate particulate formation, precipitation and sediment accumulation. Silica sols within the wetland have been subjected to variable physicochemical conditions that have at times promoted sol stability and particle growth and at other times sol destruction by flocculation and coagulation and gelation by evaporation and (or) freezing.

The unconsolidated nature of the wetland sediments contrasts strongly with deposits formed in many other sub-aqueous settings, at similar water temperatures and similar or even greater degrees of silica saturation, e.g., the shrubby precipitates within the flow path of Cistern Spring, Norris Geyser Basin (Guidry and Chafetz 2002, 2003a, 2003b). Instead, they are textually similar to particulate siliceous sediments (PSS) observed in the higher temperature vent pool environments of nonsurging, and surging nonboiling springs (Braunstein and Lowe 2001; Jones and Renaut 2003; Lowe and Braunstein 2003). The calm water conditions of the wetland and vent pools relative to the dynamic conditions of the flow path suggest that the presence or absence of turbulence that controls intercolloid–interparticle collisions and particle suspension and settling may have a major influence on precipitate fabric.

As this small wetland contains few diatoms but large volumes of unconsolidated, chemically precipitated, silica sediment, it might exemplify how silica sediments developed in these low-temperature aquatic settings prior to the advent of the diatom sink and provide an explanation for sedimentary structures that point to the presence of soft sediments preserved in the Drummond Basin and Rhynie Chert hot spring deposits. The growth, burial, and silicification of plant communities on this active geochemical wetland suggests that it has great potential as an analogue environment for the study of the plant substrate interactions, palaeoecophysiology and taphonomy of the Rhynie chert plants (Channing 2003).

The observation of unconsolidated particulate silica forming below and within water-ice formed from frozen geothermal

**Fig. 8.** Sediment accumulation and formation in sub-zero temperatures. (A) Sediment accumulation on the sinter apron of Opalescent Hot Spring, Porcelain, Basin, Norris Geyser Basin 22/4/2002. Coin for scale. (B) Fresh, unconsolidated silica sediments forming or trapped below ice in the area immediately adjacent to Porkchop Geyser's vent February 2000. (C) Area of boardwalk within the spray outfall zone of Sawmill Geyser, Upper Geyser Basin during February 2000. Water-ice formed from the spray forms a deposit several tens of centimetres thick. (D) Clumps of randomly distributed opaque silica particles up to ca. 2 cm diameter form a major component (estimated 10%–20%) of the water-ice deposit shown in C. Coin for scale.



solutions, indicates previously overlooked cold-climate silica deposition processes that may be responsible for large volume additions of particulate silica to Yellowstone hot spring environments.

### Acknowledgments

The authors would like to thank the National Park Service for permitting fieldwork and collecting in Yellowstone National Park. All staff of the Yellowstone Centre for Resources are thanked for logistical and technical assistance. Bill Wise and the interpretive staff of Norris Geyser Basin are thanked for their assistance in accessing geothermal areas. Virginia Rodrigues is thanked for water data and observations collected during the summer of 2003. We gratefully acknowledge Peter Fisher, Tony Oldroyd, Colin Lewis, Ian Butler, Ian McDonald, and Sarah Goldsmith for assistance with analytical techniques. Carolyn Davies, Lyall Anderson, and Nigel and Margie Trewin are thanked for assistance during field-

work. Nigel Trewin and Sean Guidry are acknowledged for helpful reviews of the manuscript. This study was conducted whilst AC was the recipient of Natural Environment Research Council Research Studentship GT4 97 ES.

### References

- Allen, E.T., and Day, A.L. 1935. Hot springs of the Yellowstone National Park. Carnegie Institution of Washington, Publication 466.
- Ball, J.W., McKleskey, R.B., Nordstrom, D.K., Holloway, J.M., and Verplanck, P.L. 2002. Water-chemistry data for selected springs, geysers, and streams in Yellowstone National Park, Wyoming, 1999–2000: with a section on activity of thermal features of Norris Geyser Basin, 1998 by S.A. Sturtevant. US Geological Survey, Open-file Report 02-382.
- Ball, J.W., Nordstrom, D.K., McKleskey, R.B., Schoonen, M.A.A., and Xu, Y. 2001. Water-chemistry and on-site sulfur-speciation

- data for selected springs in Yellowstone National Park, Wyoming, 1996–1998. US. Geological Survey, Open-file Report 01-49.
- Bergna, H.E. 1994. Colloid chemistry of silica: An overview. *In* The colloid chemistry of silica. *Edited by* H.E. Bergna. American Chemical Society, Advances in Chemistry Series 234, pp. 1–47.
- Braunstein, D., and Lowe, D.R. 2001. Relationship between spring and geyser activity and the deposition and morphology of high temperature (> 73 °C) siliceous sinter, Yellowstone National Park, Wyoming, U.S.A. *Journal of Sedimentary Research*, **71**: (5) 747–763.
- Bryan, S.T. 1995. The geysers of Yellowstone. University Press of Colorado, Niwot, Colo., USA.
- Channing, A. 2001. Processes and environments of vascular plant silicification. Ph.D. thesis, Cardiff University, Wales.
- Channing, A. 2003. The Rhynie Chert early land plants: palaeoecophysiological and taphonomic analogues. *Transactions of the Institution of Mining and Metallurgy, Section. B: Applied Earth Science*, **112**: B170–B171.
- Edwards, D., Kerp, H., and Hass, H. 1998. Stomata in early land plants: an anatomical and ecophysiological approach. *Journal of Experimental Botany*, **49**: 255–278.
- Everett, D.H. 1994. Basic principles of colloid science. Royal Society of Chemistry Paperbacks, London, UK.
- Fournier, R.O. 1985. The behaviour of silica in hydrothermal solutions. *In* Geology and geochemistry of epithermal systems. *Edited by* B.R. Berger and P.M. Bethke. Society of Economic Geologists, Littleton, Colo., *Reviews in Economic Geology*, Vol. 2, pp. 45–61.
- Fournier, R.O. 1989. Geochemistry and dynamics of the Yellowstone National Park hydrothermal system. *Annual Reviews in Earth and Planetary Science*, **17**: 13–53.
- Fournier, R.O., Thompson, J.M., Cunningham, C.G., and Hutchinson, R.A. 1991. Conditions leading to a recent small hydrothermal explosion at Yellowstone National Park. *Geological Society of America, Bulletin*, **103**: 1114–1120.
- Fournier, R.O., Thompson, J.M., and Hutchinson, R.A. 1992. The geochemistry of hot spring waters at Norris Geyser Basin, Yellowstone National Park. *In* Proceedings of the 7th International symposium on water rock interaction; Vol. 2, Moderate and high temperature environments. *Edited by* Y.K. Kharaka, and A.S. Maest. The International Association of Geochemistry and Cosmochemistry and The Alberta Research Council, Edmonton, Alta., Canada, 1289–1292.
- Fournier, R.O., Weltman, U., Counce, D., White, L.D., and Janik, C.J. 2002. Results of weekly chemical and isotopic monitoring of selected springs in Norris Geyser Basin, Yellowstone National Park during June–September 1995. US. Geological Survey, Open-file Report 02-344.
- Guidry, S.A., and Chafetz, H.S. 2002. Factors governing subaqueous siliceous sinter precipitation in hot springs: examples from Yellowstone National Park, U.S.A. *Sedimentology*, **49**: 1253–1267.
- Guidry, S.A., and Chafetz, H.S. 2003a. Anatomy of siliceous hot springs: examples from Yellowstone National Park, Wyoming, U.S.A. *Sedimentary Geology*, **157**: 71–106.
- Guidry, S.A., and Chafetz, H.S. 2003b. Siliceous shrubs in hot springs from Yellowstone National Park, Wyoming, U.S.A. *Canadian Journal of Earth Sciences*, **40**(11): 1571–1583.
- Hinman, N.W., and Lindstrom, R.F. 1996. Seasonal changes in silica deposition in hot spring systems. *Chemical Geology*, **132**: 237–246.
- Iler, R.K. 1979. The Chemistry of Silica: Solubility, Polymerization, Colloid and Surface Properties, and Biochemistry. John Wiley and Sons Inc., New York.
- Jones, B., and Renaut, R.W. 2003. Hot spring and geyser sinters: the integrated product of precipitation, replacement and deposition. *Canadian Journal of Earth Sciences*, **40**(11): 1549–1569.
- Kharaka, Y.K., Sorey, M.L., and Thorsden, J.J. 2000. Large-scale hydrothermal fluid discharges in the Norris–Mammoth corridor, Yellowstone National Park, U.S.A. *Journal of Geochemical Exploration*, **69–70**: 201–205.
- Lin, M.Y., Lindsay, H.M., Weitz, D.A., Ball, R.C., Klein, R., and Meakin, P. 1989. Universality in colloid aggregation. *Nature (London)*, **339**: 360–362.
- Lowe, D.R., and Braunstein, D. 2003. Microstructure of high temperature (> 73 °C) siliceous sinter deposited around hot springs and geysers, Yellowstone National Park: the role of biological and abiological processes on sedimentation. *Canadian Journal of Earth Sciences*, **40**(11): 1611–1642.
- Mountain, B.W., Benning, L.G., and Boerema, J.A. 2003. Experimental studies on New Zealand hot spring sinters: rates of growth and textural development. *Canadian Journal of Earth Sciences*, **40**(11): 1643–1667.
- Muffler, L.J.P., White, D.E., Beeson, M.H., and Truesdell, A.H. 1982. Geological map of Upper Geyser Basin Yellowstone National Park, Wyoming. US. Geological Survey, Miscellaneous Investigations Series, Map-I 1371.
- Ohsawa, S., Kawamura, T., Takamatsu, N., and Yusa, Y. 2002. Rayleigh scattering by aqueous colloidal silica as a cause for the blue colour of hydrothermal water. *Journal of Volcanology and Geothermal Research*, **113**: 49–60.
- Powell, C.L. 1994. The palaeoenvironments of the Rhynie cherts. Ph.D. thesis, University of Aberdeen.
- Powell, C.L., Trewin, N.H., and Edwards, D. 2000. Palaeoecology and plant succession in a borehole through the Rhynie cherts, Lower Old Red Sandstone, Scotland. *In* New perspectives on the Old Red Sandstone. *Edited by* P.F. Friend and B.P.J. Williams. Geological Society (of London), Special Publication 180, pp. 439–457.
- Rice, C.M., Trewin, N.H., and Anderson, L.I. 2002. Geological setting of the Early Devonian Rhynie cherts, Aberdeenshire, Scotland: an early terrestrial hot spring system. *Journal of the Geological Society, London*, **159**: 203–214.
- Rimstidt, J.D., and Cole, D.R. 1983. Geothermal Mineralisation 1: The mechanism of formation of the Beowawe, Nevada, siliceous sinter deposit. *American Journal of Science*, **283**: 861–875.
- Schreier, C. 1999. A field guide to Yellowstone's geysers, hot springs and fumaroles. Homestead Publishing, Moose, Wyo., USA.
- Trewin, N.H. 1994. Depositional environment and preservation of biota in the Lower Devonian hot springs of Rhynie, Aberdeenshire, Scotland. *Transactions of the Royal Society of Edinburgh: Earth Sciences*, **84**(3–4): 433–442.
- Trewin, N.H. 1996. The Rhynie Cherts: an early Devonian ecosystem preserved by hydrothermal activity. *In* Evolution of hydrothermal ecosystems on Earth (and Mars?). *Edited by* G.R. Bock and J. Goode. Ciba Foundation Symposium, No. 202, John Wiley and Sons Inc., New York, pp. 131–149.
- Trewin, N.H., Fayers, S.R., and Kelman, R. 2003. Subaqueous silicification of the contents of small ponds in an Early Devonian hot spring complex, Rhynie, Scotland. *Canadian Journal of Earth Sciences*, **40**(11): 1697–1712.
- Vinson, D.K., and Rushforth, S.R. 1989. Diatoms species composition along a thermal gradient in the Portneuf River, Idaho, U.S.A. *Hydrobiologia*, **185**: 41–54.
- Walter, M.R. 1976. Hot spring sediments in Yellowstone National

- Park. *In* *Stromatolites: Developments in Sedimentology*, Edited by M.R. Walter. Elsevier, Amsterdam, The Netherlands, Vol. 20, pp. 489–498.
- Walter, M.R., and Des Marais, D.J. 1993. Preservation of biological information in thermal spring deposits: developing a strategy for the search for fossil life on Mars. *Icarus*, **101**: 129–143.
- Walter, M.R., Des Marais, D., Farmer, J.D., and Hinman, N.W. 1996. Lithofacies and biofacies of mid-Paleozoic thermal spring deposits in the Drummond Basin, Queensland, Australia. *Palaios*, **11**: 497–518.
- Walter, M.R., McLoughlin, S., Drinnan, A.N., and Farmer, J.D. 1998. Palaeontology of Devonian thermal spring deposits, Drummond Basin, Australia. *Alcheringa*, **22**: 285–314.
- Weed, W.H. 1889. Formation of travertine and siliceous sinter by the vegetation of hot springs. *In* US. Geological Survey, Washington D.C., Annual Report 9. pp. 613–676.
- White, D.E., Hutchinson, R.A., and Keith, T.E.C. 1988. The geology and remarkable thermal activity of Norris Geyser Basin, Yellowstone National Park, Wyoming. US. Geological Survey, Professional Paper 1456.
- White, N.C., Wood, D.G., and Lee, M.C. 1989. Epithermal sinters of Paleozoic age in north Queensland, Australia. *Geology*, **17**: 718–722.
- Williams, L.A., and Crerar, D.A. 1985. Silica diagenesis, II. General mechanisms. *Journal of Sedimentary Petrology*, **55**(3): 0312–0321.
- Yee, N., Phoenix, V.R., Konhauser, K.O., Benning, L.G., and Ferris, F.G. 2003. The effect of cyanobacteria on Si precipitation kinetics at neutral pH: Implications for bacterial silicification in geothermal hot springs. *Chemical Geology*, **99**: 83–90.